Journal of Dental Sciences 17 (2022) 696–706

Available online at www.sciencedirect.com

ScienceDirect

journal homepage: www.e-jds.com

Original Article

Co-upregulation of *miR-31* and its host gene lncRNA *MIR31HG* in oral squamous cell carcinoma

Hsi-Feng Tu [a,b,c*], Chung-Ji Liu [a,d], Wan-Wen Hung [b], Tzong-Ming Shieh [e]

[a] *Department of Dentistry, College of Dentistry, National Yang Ming Chiao Tung University, Taipei, Taiwan*
[b] *Institute of Oral Biology, College of Dentistry, National Yang Ming Chiao Tung University, Taipei, Taiwan*
[c] *Department of Stomatology, National Yang Ming Chiao Tung University Hospital, Yi-Lan, Taiwan*
[d] *Department of Dentistry, Taipei MacKay Memorial Hospital, Taipei, Taiwan*
[e] *Department of Dentistry, College of Dentistry, China Medical University, Taichung, Taiwan*

Received 3 November 2021; Final revision received 7 November 2021
Available online 27 November 2021

KEYWORDS
Carcinoma;
miR-31;
MIR31HG;
Mouth;
Oral

Abstract *Background/purpose:* Several long non-coding RNAs (lncRNAs) harbor miRNA in their genome. MIR31HG harbors miR-31 in its intron and it is speculated that they are co-expressed in tumors. This study addressed whether frequent miR-31 and MIR31HG co-upregulation occurred in oral squamous cell carcinoma (OSCC) and its clinical implications.
Materials and methods: Microarray was performed to retrieve dis-regulated lncRNAs from tissue sample. The ectopic gene expression was carried out to specify the phenotypic influences of selected lncRNA screened from bioinformatic algorithms. The expression of *miR-31* and *MIR31HG* in tissues or scrapped samples was analyzed using qRT-PCR. The implications of gene expression as related to metastasis or survival were further dissected.
Results: Microarray identified disrupted transcripts including *MIR31HG* and other 152 lncRNAs aberrantly expressed in OSCC tissues. *In silico* algorithms annotated an eminent involvement of aberrant transcripts in the regulation of cell cycle, extracellular modulation, adhesion, and wound healing. The enhancement of proliferation, wound healing, invasion and anchorage-independent colony formation mediated by *MIR31HG* was ascertained by ectopic expression in OECM1 cells. Besides, co-upregulation of *miR-31* and *MIR31HG* was conspicuous in OSCC tissues. High expression of *miR-31* and *MIR31HG* designated a trend of worse OSCC prognosis. Interestingly, high *MIR31HG* expression defined a very poor survival in stage IV diseases. By contrast, high *miR-31* expression predicted nodal metastasis in stage I–III diseases.
Conclusion: Assessment of miR-31 and MIR31HG expression in OSCC may enable the prognostic

* Corresponding author. Department of Dentistry, College of Dentistry, National Yang Ming Chiao Tung University, Taipei, 11211, Taiwan.
E-mail addresses: hftu@nycu.edu.tw, hftu@nycu.edu.tw (H.-F. Tu).

https://doi.org/10.1016/j.jds.2021.11.006
1991-7902/© 2021 Association for Dental Sciences of the Republic of China. Publishing services by Elsevier B.V. This is an open access article under the CC BY-NC-ND license (http://creativecommons.org/licenses/by-nc-nd/4.0/).

prediction. The candidate lncRNAs isolated from this work can be further validated as crucial factors contributing to OSCC pathogenesis.
© 2021 Association for Dental Sciences of the Republic of China. Publishing services by Elsevier B.V. This is an open access article under the CC BY-NC-ND license (http://creativecommons.org/licenses/by-nc-nd/4.0/).

Introduction

In human, the coding region comprised only 1.2% of the whole genome.[1] The other part of the non-coding regions was previously considered as less important although they make up the majority of genome. The biological function of the non-coding region and their transcriptome draws attention in recent years. As the advancement of whole genome sequencing technology, more and more studies showed that mutations occurred not only in coding region but also in non-coding region, moreover around 80% cancer-related SNPs were found in non-coding region.[1] According to size, these non-coding RNA can be divided into two category, long non-coding RNA (lncRNA; >200 bp) and small non-coding RNA(<200 bp). Small non-coding RNAs like microRNAs (miRNA) are thoroughly identified and characterized. And their function in translation repression is also well studied. However, complicated biologic activity of lncRNA is still under investigation. Most lncRNAs are transcribed by RNA polymerase II, hence their structures are similar to mRNA. Studies have shown the comprehensive role of lncRNAs in epigenetic, transcriptional, post-transcriptional, and translation regulation, as well as post-translational modification.[2] The interactive functions of lncRNA are more complicated than expected.

In Taiwan, the prevalence of areca chewing accounts for the high incidence of oral squamous cell carcinoma (OSCC) among male adults. The areca quid mainly consists of betel leaf, areca nut and slaked lime. These ingredients, especially areca nut, exert carcinogenesis potential by direct and indirect genotoxicity.[3,4] The genomic signature of mismatch repair deficiency has also been identified in areca related OSCC tissues.[5] Recent study also showed that areca induced whole transcriptome changes associated with diabetes, obesity and metabolic syndrome in a human monocyte cell line.[6] Despites the coding transcriptome change, the importance of non-coding transcriptome aberrance attracts more attention in recent days. miRNAs have high specificity of expression in certain tissues and disease. Studies also demonstrated that miRNA expression profiles have better accuracy in disease classification than mRNA.[7,8] Recent microarray profiling identified a set of 105 miRNAs with altered expressed in OSCC and qPCR validation revealed that up-regulation of *miR-196a*, *miR-21*, *miR-1237* and down-regulation of *miR-204*, *miR-144* was associated with poor prognosis of OSCC. The *miR-196a*/*miR-204* ratio served as a good predictor for disease recurrence and survival.[9] Our previous studies have demonstrated the important role of *miR-21* and *miR-31* during oral carcinogenesis.[10,11] The upregulation of *miR-372*/*373* was observed correlated to lymph node metastasis OSCC.[12] It is worthy noted that interactions between miRNA and lncRNA are demonstrated and many lncRNAs function as competing endogenous RNAs (ceRNA). LncRNA *IUR* and *MEG3* could sponge *miR-21* and neutralize the oncogenic effect of *miR-21*.[13,14] LncRNA *FER1L4* is a ceRNA to binding with *miR-372*, which results in E2F1 up-regulation and proliferative promotion of glioma cells.[15] Certain lncRNAs are also identified as host gene for miRNA. The *miR-497* and *miR-195* were derived from lncRNA *MIR497HG*. The *MIR497HG* together with *miR-497* and *miR-195*, were downregulated in bladder cancer, and the expression of *MIR497HG* could suppress the progression of bladder cancer cells.[16] Copy number deletion of the *MIR99-AHG* gene was observed in lung adenocarcinoma, which led to the downregulation of its four transcripts: lncRNA *MIR99AHG* and the *miR-99a*/*let-7c*/*miR-125b2* cluster. Further experiments also confirmed the suppressor role of *MIR99AHG* and *miR-99a*.[17]

MIR31HG, a host gene of an important oncomir *miR-31*, was found in both nucleus and cytoplasm under normal condition, but *MIR31HG* and *miR-31* were exported to cytoplasm following oncogene B-RAF induction. *MIR31HG* is upregulated in oncogene induced senescence and negatively regulates tumor suppressor p16.[18] *MIR31HG* could also targets HIF1A and p21 and promote cell cycle progression in head and neck cancer cells.[19] However, the expression of *MIR31HG* was negatively correlated to overall survival of lung adenocarcinoma, but it was a favorable prognostic factor in gastrointestinal cancer.[20] In this study, we identified the expression profile of lncRNA in areca-related oral carcinogenesis. The expression and clinical implications of MIR31HG in OSCC were also investigated.

Materials and methods

Subjects

The primary OSCC tumors and their paired non-cancerous matched tissue samples were derived from 40 patients (Table 1). Samples were collected after obtaining written informed consent. The study was approved by IRB committee of National Yang-Ming University Hospital and Taipei Mackay Memorial Hospital with approval numbers NYMUH 2014A002 and 17MMHIS053/18MMHIS176, respectively.

Swabbed samples were collected from lesion and normal looking control mucosa from OSCC patients in National Yang-Ming University Hospital or Taipei MacKay Memorial Hospital with IRB approval numbers of NYMUH2019A013 and 18MMHIS187e, respectively. A Libo specimen collection swab (Cat No. 30221.3, Iron Will, New Taipei City, Taiwan) was used to achieve scrapped cells. The detailed sampling procedures and analysis followed the protocols established in previous study.[21]

Table 1 Clinical parameters of OSCC samples.

n = 40	
Age (mean ± SEM)	57.53 ± 1.58
Gender (male/female)	36/4
Areca chewing	30
Tobacco smoking	30
T1−3	15
T4	25
N0	26
N+	14
Stage I−III	12
Stage IV	28
Follow-up (mean ± SEM, days)	2810 ± 227.1
Death	10
Alive	30

LncRNA microarray

Total RNA was amplified by a Low Input Quick-Amp Labeling kit (Agilent Technologies, Santa Clara, CA, USA) and labeled with Cy3 (CyDye, Agilent Technologies) during the *in vitro* transcription process. The Cy3-labled cRNA was fragmented to an average size of about 50−100 nucleotides by incubation with fragmentation buffer at 60 °C for 30 min. Corresponding fragmented labeled cRNA was then pooled and hybridized to Agilent SurePrint G3 Human Gene Exp V3 8 × 60K Microarray (Agilent Technologies) at 65 °C for 17 h. After washing and drying by nitrogen gun blowing, microarrays were scanned with an Agilent microarray scanner (Agilent Technologies) at 535 nm for Cy3. Scanned images were analyzed by Feature extraction10.5.1.1 software (Agilent Technologies), an image analysis and normalization software were used to quantify signal and background intensity for each feature.

Bioinformatic analysis

The Venn diagram and gene annotation analysis of microarray data were performed using web-based resources (https://metascape.org/gp/index.html#/main/step1).[22] From microarray data, we selected genes with expression change more than and less than two folds for further analysis. Venn diagrams represent the overlapping of genes between samples whereas circoplots demonstrate their relationships. The cluster analysis was also performed using a web-based heatmap visualization and analysis tool clustergrammer.[23] The non-supervised cluster analysis was performed on 153 overlapping lncRNAs and also the top 50 dysregulated lncRNAs.

Cell culture, plasmid construction and phenotypic assays

The OECM1 OSCC cell line was cultured as previously described.[24] The lentiviruses containing *MIR31HG* transcript cloned in the pLV-EF1a-GFP vector and control virus are gifts from Professor Shu-Chun Lin. OECM1 was infected with virus and selected to achieve stable cell sublines with *MIR31HG* expression.[25] Cell proliferation, wound closure, transwell invasion and anchorage-independent colony formation assays, and were carried out according to previously published protocols.[24,25]

Quantitative polymerase chain reaction (qPCR) analysis

TaqMan miRNA assay kits and qPCR probes obtained from Apply Biosystems (Waltham, MA, USA) were used to quantify the expression of *MIR31HG* and *miR-31* using *GAPDH* or *RNU6B* as internal controls.[24,25] The Cat. No. of each probe was Hs01107339_gl, 002279, Hs00266705_gl and 001093, respectively. $-\Delta Ct$ is the difference in threshold cycle number across the test gene and the internal control. $-\Delta\Delta Ct$ indicates the difference in $-\Delta Ct$ across the test and the control group. $2^{-\Delta\Delta Ct}$ designates the fold change in gene expression relative to control.[24]

Statistics

Mann−Whitney tests, *t*-tests, two-way ANOVA test, linear correlation analysis and Kaplan−Meier survival analysis were performed. A receiver operating characteristic (ROC) curve was used to acquire area under curve (AUC), sensitivity and specificity of variables to evaluate separation power.[21]

Results

Gene expression profile from areca-associated OSCCs

To determine the gene expression profile of areca-related OSCC, normal and cancer tissue pairs from three patients were utilized for microarray analysis. The Agilent SurePrint G3 Human Gene Exp V3 8 × 60K Microarray could detect 30,600 lncRNAs and 26,100 coding genes. Among three cases, two were stage I tumors and one was stage IV disease with lymph node metastasis in neck (Fig. 1A). The gene expression level from normal to tumor were analyzed and genes with more than or less than two-fold changes were counted. The Venn diagram demonstrated the overlap of counted genes between three cases and around 2050 common genes were identified in all three cases (Fig. 1B). Case 1 and case 2 are stage I disease and they shared more common genes than either one comparing to case 3 advanced tumor. The discrepancies were also noted in Circos plot (Fig. 1C). Gene ontology (GO) analysis performed on 2050 common genes annotated the most significant involved pathway was cycle related. It was followed by extracellular matrix related, cell adhesion pathways or responses to wounding, which were important pathways during carcinogenesis (Fig. 1D).

lncRNA expression profile from areca-associated OSCCs

The microarray comprised 30600 lncRNAs and only lncRNA with more than or less than two-fold expression change

A

	Gender	Age	TNM	Site
Case 1	M	56	T1N0M0	Mouth floor
Case 2	M	53	T1N0M0	Tongue
Case 3	M	44	T2N2bM0	Tongue

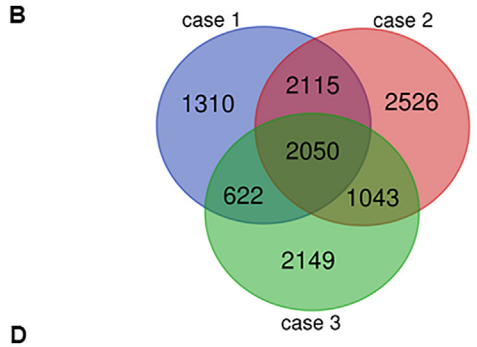

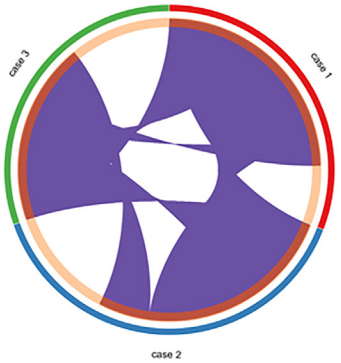

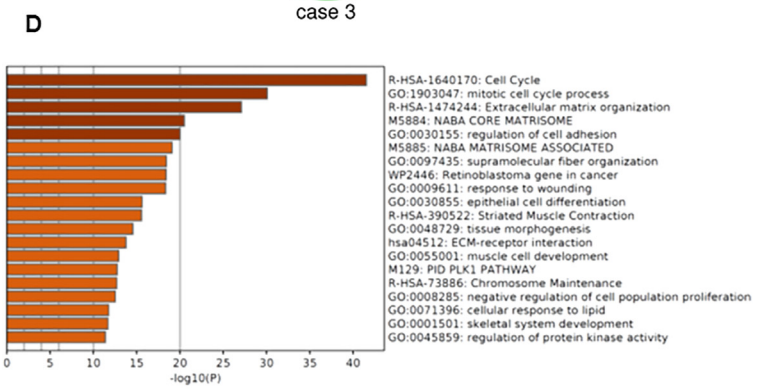

Figure 1 Microarray analysis of OSCC tumors. (A) The clinical parameters of cases. (B) Venn diagram to show the genes aberrantly expressed for at least two folds. (C). Circos plot to show the higher similarity between case 1 and case 2 in the gene dis-regulation, which separates from those in case 3. (D) GO annotation to show the disrupted pathways.

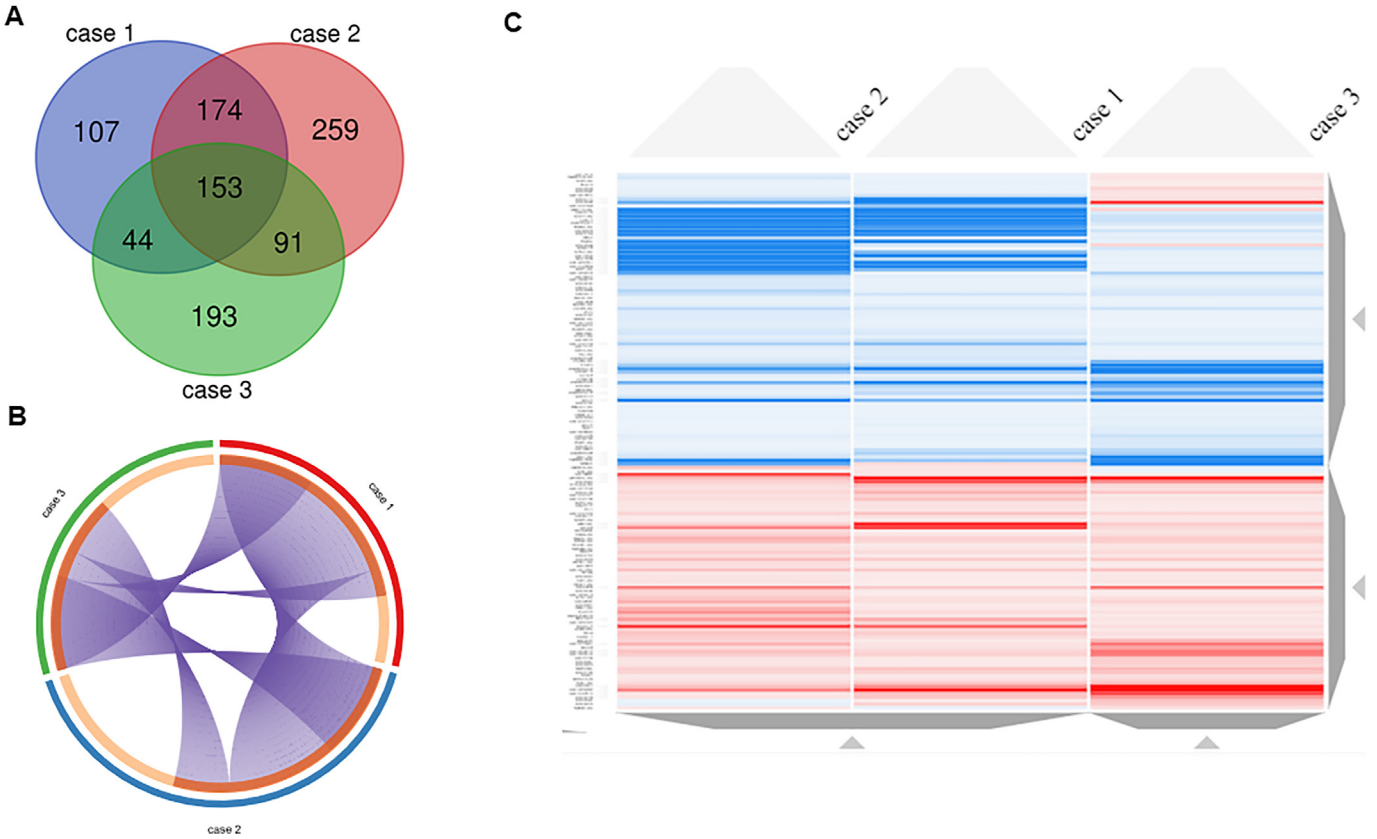

Figure 2 The dis-regulation of lncRNAs in microarray analysis. (A) Venn diagram to show the lncRNAs aberrantly expressed for at least two folds. (B) Circos plot to show the higher similarity and interaction in the lncRNA dis-regulation between case 1 and case 2, comparing to case 3. (C) Heatmap of cluster analysis according to 153 lncRNAs commonly present in three tumors. The similarity between case 1 and case 2 is still higher than case 3. Blue, Down-regulated; red. Up-regulated.

A

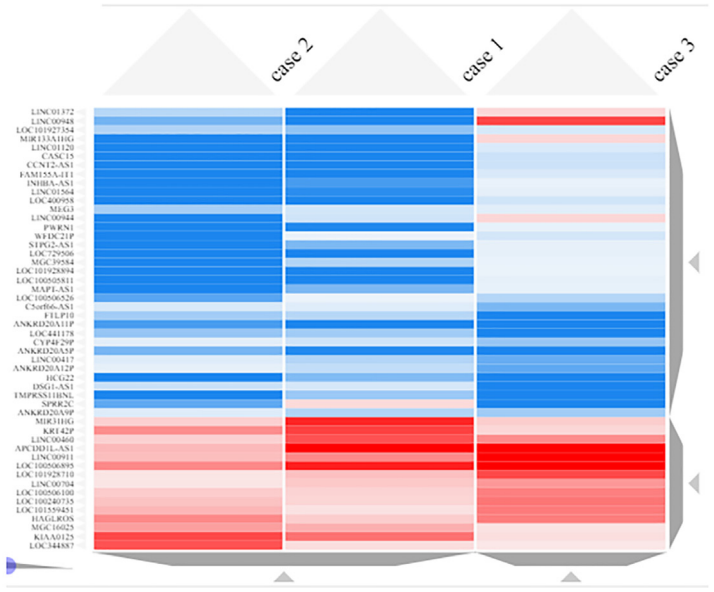

B

lncRNA

Down-regulated		Up-regulated
MAPT-AS1	STPG2-AS1	HAGLROS
LINC01564	LOC101928894	KRT42P
LINC01120	TMPRSS11BNL	LOC101928710
ANKRD20A11P	MGC39584	LINC00460
MIR133A1HG	C5ORF66-AS1	APCDD1L-AS1
WFDC21P	CCNT2-AS1	LOC344887
LOC101927354	LOC729506	LOC101559451
DSG1-AS1	ANKRD20A5P	LOC100240735
LINC00948	LOC100506526	MGC16025
FAM155A-IT1	INHBA-AS1	LOC100506100
LINC00944	LINC00417	LINC00704
HCG22	LOC100505811	KIAA0125
ANKRD20A12P	PWRN1	LINC00911
LOC400958	SPRR2C	LOC100506895
FTLP10	CASC15	MIR31HG
LINC01372	ANKRD20A9P	
CYP4F29P	LOC441178	
MEG3		

Figure 3 The top 50 dis-regulated lncRNAs. (A) Heatmap of cluster analysis. (B). The illustration of aberrant lncRNAs. Blue, Down-regulated; red. Up-regulated.

from normal to tumor counterpart were selected. There are 478 altered lncRNAs identified in case 1, 677 in case 2, and 481 in case 3. A total of 153 common lncRNAs existing in three cases were showed in Venn diagram (Fig. 2A). The Circo plot analysis revealed the pattern of correlation between 3 cases and the lncRNA expression profile are more similar between case 1 and case 2, which resembles the profile of the whole gene set as mentioned above (Fig. 2B). The heatmap demonstrated the up-regulated (red) and down-regulated (blue) lncRNAs from normal to tumor. Non-supervised cluster analysis confirmed the different expression profile between case 3 and the remains (Fig. 2C). Moreover, if we select the top 50 dys-regulated lncRNAs among three cases, down-regulated lncRNAs outnumber the up-regulated ones (Fig. 3A). Most of dysregulated lncRNAs are RNA genes but some belong to pseudogenes and some are miRNA host genes. Among up-regulated lncRNAs, for example, LOC344887, KIAA0125 were reported correlated with oncogenic activity and stemness.[26,27] Interestingly, the non-supervised cluster analysis identified *MIR31HG* as significant up-regulated lncRNA among top 50 dysregulated lncRNA (Fig. 3B).

MIR31HG influences the oncogenicity of OECM1 cell

To determine the phenotype exerted by *MIR31HG*, OECM1 OSCC cell line, an areca-chewing related cell line, was selected for *MIR31HG* overexpression experiments. Lentivirus carrying *MIR31HG* expression construct was introduced into OECM1 cells through infection. The high infection efficiency was noted in the selected subline (Fig. 4A), and this subline had a stable and robust *MIR31HG* expression (Fig. 4B). Proliferation assay demonstrated the growth advantage in *MIR31HG* expression cells (Fig. 4C). Enhanced migration ability was also noted in wound healing assay and invasion assay (Fig. 4D and E). Anchorage-independent colony formation assay revealed the increased *in vitro* oncogenic potential as related to *MIR31HG* expression (Fig. 4F). The results suggest an oncogenic role of *MIR31HG* in OSCC, and the expression profile of *MIR31HG* and its hosted *miR-31* in OSCC tissue was further studied thereafter.

Validation of MIR31HG expression in OSCCs

Among 40 OSCC patients enrolled for tissue study 75% (30/40) patients had areca chewing habits (Table 1). The expression of *MIR31HG* and *miR-31* were determined by qPCR. A significantly up-regulated in *MIR31HG* expression from normal to tumor were found, and the upregulation of *miR-31* expression was more conspicuous (Fig. 5A and B). Correlation analysis also showed a significantly positive correlation between *MIR31HG* and *miR-31* expression (Fig. 5C). In a series of brushing samples from 10 OSCC patients, the expression of *MIR31HG* was significantly up-regulated from normal to tumor counterpart (Fig. 5D). The qPCR results were in line with lncRNA microarray findings, which substantiate the expression of *MIR31HG* could be a biomarker like *miR-31* being previously detected in OSCC.

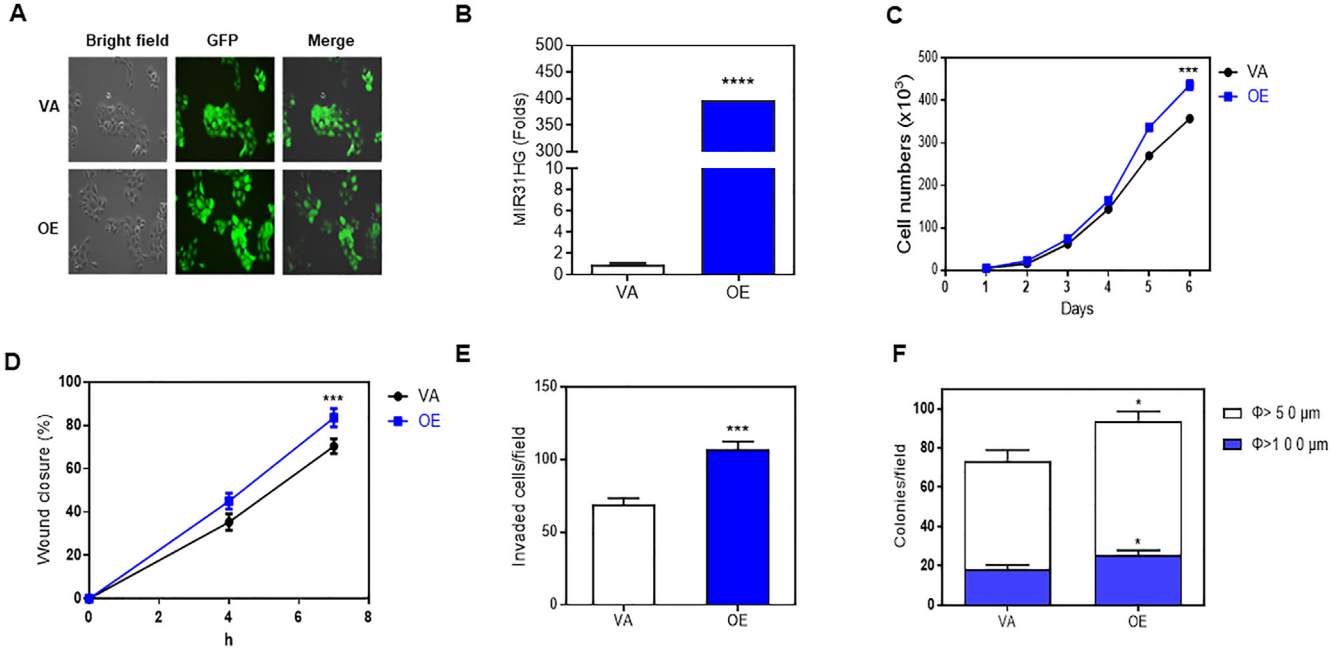

Figure 4 Exogenous *MIR31HG* expression in OECM1 cells. (A) Both cell subline with ectopic *MIR31HG* expression and control cell subline exhibit green fluorescence (×200). VA, vector alone control. OE, *MIR31HG* expression. (B) *MIR31HG* expression drastically increases in OE relative to VA. (C—F) OE cells exhibit an increased proliferation (in C), wound closure rate (in D), invasion (in E) and anchorage-independent colony formation ability (in F) relative to VA cells. *ns*, not significant; *, $p < 0.05$, **, $p < 0.01$ and ***, $p < 0.001$. Mann—Whitney test or two-way Anova test.

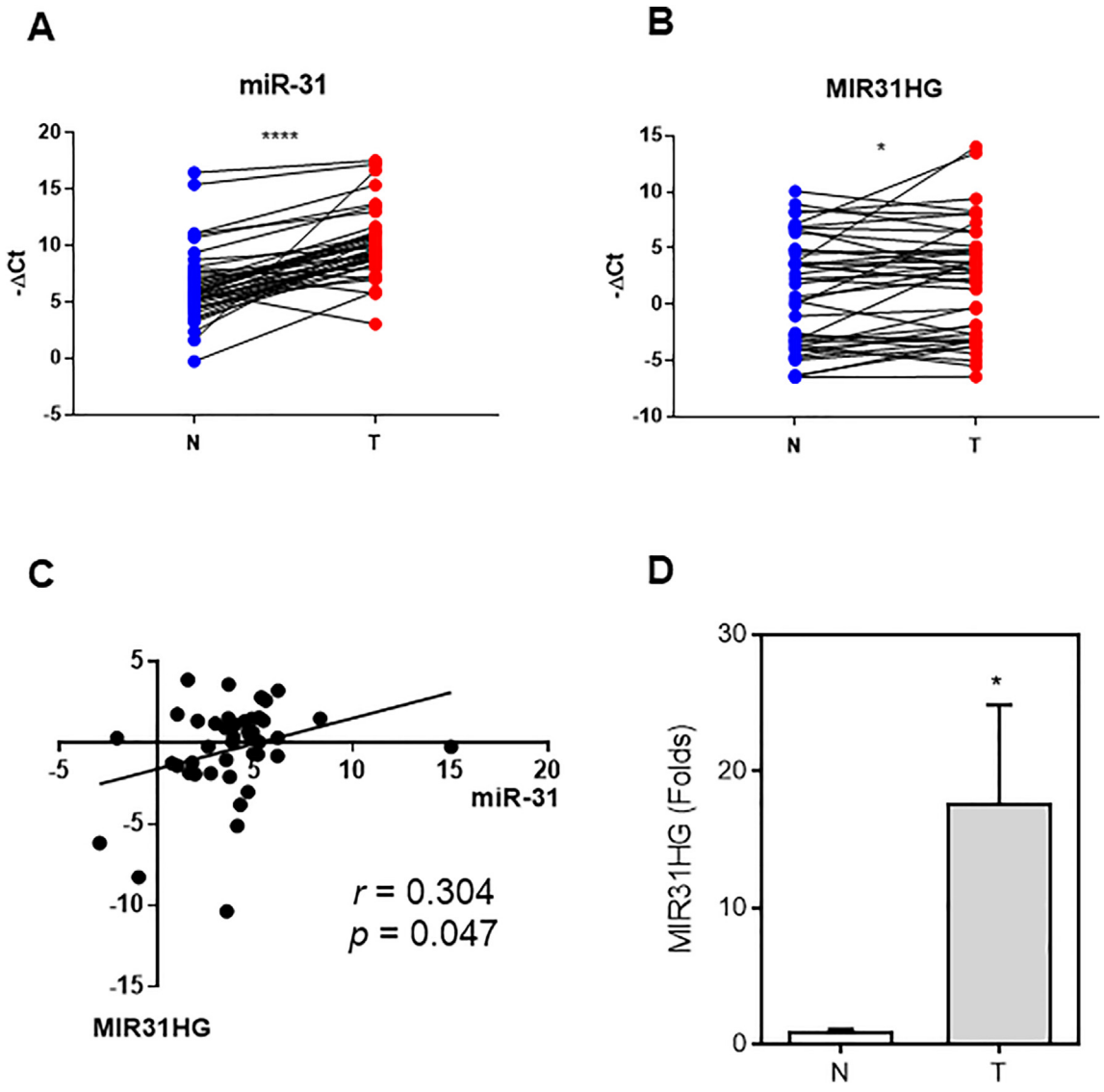

Figure 5 qPCR analysis. (A–B) Analysis of OSCC tissue pairs. (A, B) Before–after plots of *miR-31* and *MIR31HG*, respectively. Y axis, −ΔCt. (C). Linear correlation analysis according to −ΔΔCt. (C) Analysis of *MIR31HG* expression in swabbed samples. Bar chart, mean ± SE. (A, B, D) Paired-*t*-test. N, normal control; T, OSCC. *, $p < 0.05$ and ****, $p < 0.0001$.

Prognostic value of MIR31HG and miR-31 expression in OSCCs

We assessed the prognosis value of *MIR31HG* and *miR-31* in our patients who had been followed for an average of 2810 days (Table 1). Among them, 10 subjects were dead during follow-up. Initially, the ROC analysis was performed with the classification variable as survival to yield a cut-off value, which could discriminate the expression states of *MIR31HG* or *miR-31* into high or low. The Kaplan–Meier analysis revealed a trend that patients with higher *MIR31HG* expression had poor survival, however, the differences was not statistically significant (Fig. 6A). Similar trend was found in *miR-31* expression (Fig. 6B). Further dissection revealed that patients had both high *MIR31HG* and high *miR-31* expression exhibiting worsened survival (Fig. 6C). Moreover, in stage IV patients, the expression of *MIR31HG* seemed to be a potent prognosis marker (Fig. 6D).

The neck nodal metastasis prediction is a critical issue in OSCC treatment. We performed ROC analysis to determine whether *MIR31HG* or *miR-31* expression could predict nodal metastasis. Interesting, *miR*-31 has an AUC of 0.65 to diagnose nodal metastasis, which is much better than *MIR31HG* (Fig. 7A and B). Of note, in stage I–III diseases that neck dissection is sometimes optional, the prediction of nodal metastasis appeared useful as that *miR-31* expression could significantly distinguish the nodal metastasis among stage I–III patients (Fig. 7C). The findings warranted a future clinical application in terms of *miR-31* expression.

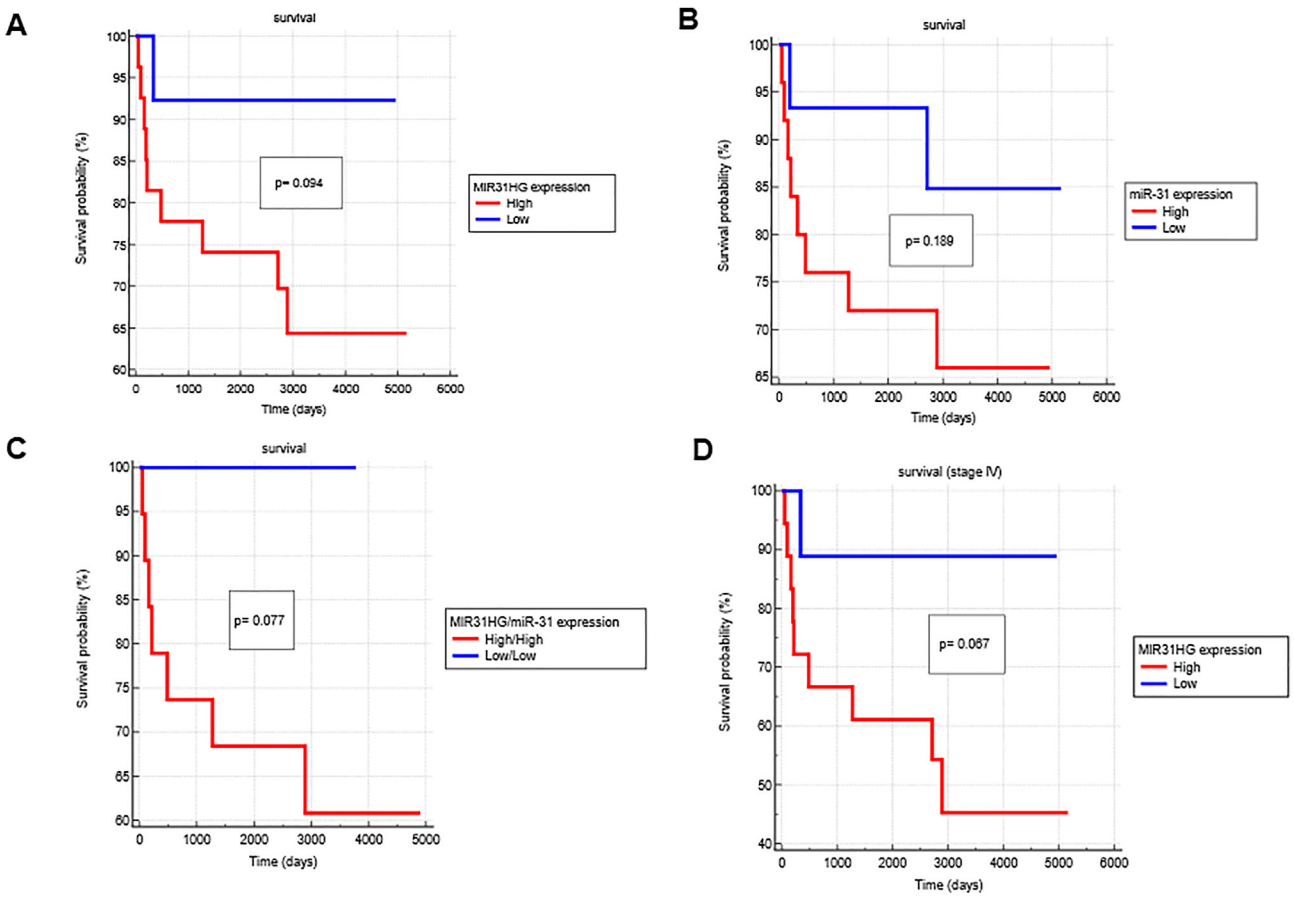

Figure 6 Kaplan—Meier survival analysis. (A—C) All tumors. (A) *MIR31HG*, (B) *miR-31*, (C) both *MIR31HG* and *miR-31*. (D) Stage IV tumors/*MIR31HG*. Cut off values of $-\Delta\Delta$Ct achieved from preliminary tests is used to divide tumors with high or low expression.

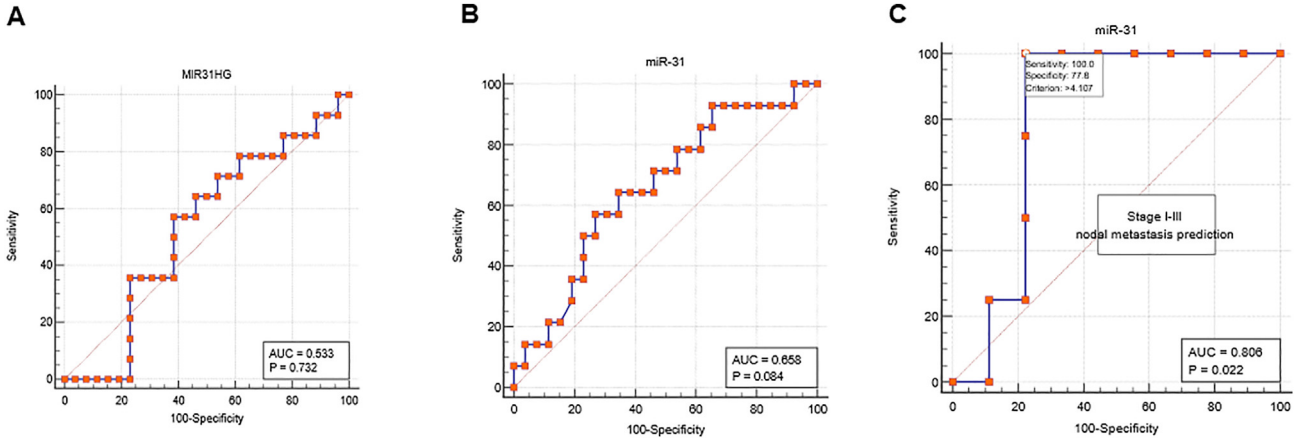

Figure 7 Receiver Operating Characteristic curves of $-\Delta\Delta$Ct to distinguish nodal metastasis of tumors. (A, B) All tumors. (A) *MIR31HG*, (B) *miR-31*. (C) Stage I—III tumors/*miR-31*. *miR-31* expression enables the separation of metastasis *vs* non-metastasis in non-stage IV tumors.

Discussion

Although the biological functions of lncRNA are not very diverse, their abundance in transcriptome warrants the potential role in carcinogenesis. Our lncRNA microarray results revealed a panel of dysregulated lncRNAs with novelty. Among up-regulated lncRNAs, *HAGLROS* is a STAT3-induced lncRNA that contributes to the malignant progression of gastric cancer.[28] *HAGLROS* could sponge *miR-152* and up-regulate ROCK1 expression in osteosarcoma.[29] In lung cancer, *LINC00460* promotes epithelial–mesenchymal transition and cell migration.[30] *LINC00460* also enhances bladder carcinoma cell proliferation and migration by modulating *miR-612/FOXK1* Axis.[31] *KRT42P* is a pseudogene with unknown function. *LOC100506100*, *LOC101928710*, *LOC101559451*, *LOC100240735* and *MGC16025* are all uncharacterized lncRNAs. Intriguingly, *LOC100506100* is the lncRNA most profoundly up-regulated in our samples. The down-regulated lncRNAs outnumber the up-regulated lncRNAs in our data, which might imply that more lncRNA may drive suppressive influences. Study has shown that approximately 60% of the protein-coding genes are targeted by miRNA, whereas 70% protein coding genes are targeted by lncRNA.[32] Since lncRNA could act as miRNA sponge, the interplay between coding RNAs and non-coding RNAs is far more complicated than expected.

In the perspective of biomarker detection, up-regulation molecule is a better candidate than down-regulation ones. We thus focus on the lncRNAs which were up-regulated in cancer tissues and identify *MIR31HG* as an important oncogenic lncRNA. *MIR31HG* genome located on 9p21 and the gene locus is chr9:21,439,475-21,591,766(GRCh38/hg38) consisting of 152,292 nucleotides. The 2166 bp *MIR31HG* transcript composed of four exons is identified later on a non-coding RNA. In RNAseq analysis, *MIR31HG* is abundant in gastrointestinal tract compared to other part of human body,[33] whereas it seems that the survival prediction of *MIR31HG* may vary according to cancer type.[34] Our data signifies that *MIR31HG* expression might correlate with overall survival of OSCC patients, especially in late-stage disease. Similar result has been noted in laryngeal SCC that *MIR31HG* overexpression represents poor prognosis, and *MIR31HG* could negatively target p21 to facilitate the progression of cell cycle.[19] Our *in vitro* results showed the enrichment in cell proliferation after *MIR31HG* expression. Furthermore, since our annotations of microarray data revealed that cell cycle related pathway are the most involved ones, the findings on proliferative enhancement together with the promotion on other phenotypes mediated by *MIR31HG* expression is compatible with *in silico* prediction. Through the alternative splicing, *MIR31HG* transcript comprises 4 exons, and *miR-31* is localized in intron 1. It is speculated that these two non-coding transcripts could be generated together in cells. In colorectal carcinoma samples, a strong correlation between *miR-31* and *MIR31HG* was shown (Spearman's $r > 0.80$).[35] Both *miR-31* and *MIR31HG* have been known up-regulated in oral precancerous lesions.[21,25] In our OSCC patient cohort, the co-upregulation of them was also demonstrated (Spearman's $r > 0.3$). Since bioinformatics studies predicted that approximately 20% of intronic miRNAs target host mRNA transcripts in a feedback loop,[36] *miR-31* and *MIR31HG* might share the coordinative modulation in oncogenesis.

Although the power in survival prediction is not as good as *MIR31HG*, *miR-31* expression seems to correlated more with neck nodal metastasis. Distinct gene expression profile among nodal positive and nodal negative cases was reported.[37] Similar result was preliminarily noticed in our microarray data. Only case 3 has nodal metastasis. Although case 2 and case 3 are all tongue cancers, cluster analysis of gene expression profile separated case 3 from case 1 and case 2. Most importantly, our data showed that *miR-31* expression could predict the nodal metastasis in stage I–III patients (AUC:0.8, sensitivity 100%, specificity 78%). The findings could assist the therapeutic decision for neck lymph node dissection in early-stage patients. Novel downstream target of *MIR31HG* such as *LBH* has been identified recently,[25] whereas, the upstream promoter control of *MIR31HG* could be as complicated as downstream effects. Previous study has shown that EGF up-regulates *miR-31* through the C/EBPβ signal cascade.[38] *MIR31HG* could also be negatively regulated by *miR-193b*.[39] However, the regulatory mechanism of and *MIR31HG* and *miR-31*co-upregulation in areca-related OSCC needs further elucidation. The interactive roles that *MIR31HG* and *miR-31* co-plays in OSCC pathogenesis require specification. To resolute the functions of uncharacterized lncRNAs may bestow novel mechanistic insights in neoplastic process.

Declaration of competing interest

The authors have no conflicts of interest relevant to this article.

Acknowledgments

We acknowledge the helps from Professors Shu-Chun Lin and Kuo-Wei Chang. This work is supported by grants RD2015003, RD2016003 and RD2018003 from NYMUH and MOST107-2314-B-010-026-MY3 and MOST107-2314-B-010-031 from Ministry of Science and Technology, Taiwan.

References

1. Dunham I, Kundaje A, Aldred SF, et al. An integrated encyclopedia of DNA elements in the human genome. *Nature* 2012;489:57–74.
2. Zhang X, Wang W, Zhu W, et al. Mechanisms and functions of long non-coding RNAs at multiple regulatory levels. *Int J Mol Sci* 2019;20:5573–602.
3. Chen P-H, Mahmood Q, Mariottini GL, Chiang T-A, Lee K-W. Adverse health effects of betel quid and the risk of oral and pharyngeal cancers. *BioMed Res Int* 2017;2017:3904098.
4. Ko YC, Huang YL, Lee CH, Chen MJ, Lin LM, Tsai CC. Betel quid chewing, cigarette smoking and alcohol consumption related to oral cancer in taiwan. *J Oral Pathol Med* 1995;24:450–3.
5. Yang WF, Qin N, Song X, et al. Genomic signature of mismatch repair deficiency in areca nut-related oral cancer. *J Dent Res* 2020;99:1252–61.
6. Cardoso S, Ogunkolade BW, Lowe R, et al. Areca catchu-(betel-nut)-induced whole transcriptome changes associated with diabetes, obesity and metabolic syndrome in a human monocyte cell line. *BMC Endocr Disord* 2021;21:165–76.

7. Lu J, Getz G, Miska EA, et al. MicroRNA expression profiles classify human cancers. *Nature* 2005;435:834—8.
8. Søkilde R, Persson H, Ehinger A, et al. Refinement of breast cancer molecular classification by miRNA expression profiles. *BMC Genom* 2019;20:503—14.
9. Rajan C, Roshan VGD, Khan I, et al. MiRNA expression profiling and emergence of new prognostic signature for oral squamous cell carcinoma. *Sci Rep* 2021;11:7298—309.
10. Yu EH, Tu HF, Wu CH, Yang CC, Chang KW. MicroRNA-21 promotes perineural invasion and impacts survival in patients with oral carcinoma. *J Chin Med Assoc* 2017;80:383—8.
11. Hung KF, Liu CJ, Chiu PC, et al. MicroRNA-31 upregulation predicts increased risk of progression of oral potentially malignant disorder. *Oral Oncol* 2016;53:42—7.
12. Tu HF, Chang KW, Cheng HW, Liu CJ. Upregulation of miR-372 and -373 associates with lymph node metastasis and poor prognosis of oral carcinomas. *Laryngoscope* 2015;125:E365—70.
13. Wang B, Hua P, Zhang L, Li J, Zhang Y. LncRNA-IUR up-regulates PTEN by sponging miR-21 to regulate cancer cell proliferation and apoptosis in esophageal squamous cell carcinoma. *Esophagus* 2020;17:298—304.
14. Jia HY, Zhang K, Lu WJ, Xu GW, Zhang JF, Tang ZL. LncRNA MEG3 influences the proliferation and apoptosis of psoriasis epidermal cells by targeting miR-21/caspase-8. *BMC Mol Cell Biol* 2019;20:46—58.
15. Xia L, Nie D, Wang G, Sun C, Chen G. FER1L4/miR-372/E2F1 works as a cerna system to regulate the proliferation and cell cycle of glioma cells. *J Cell Mol Med* 2019;23:3224—33.
16. Zhuang C, Liu Y, Fu S, et al. Silencing of lncRNA MIR497HG via CRISPR/CAS13d induces bladder cancer progression through promoting the crosstalk between Hippo/Yap and TGF-β/Smad signaling. *Front Mol Biosci* 2020;7:616768.
17. Han C, Li H, Ma Z, et al. MIR99AHG is a noncoding tumor suppressor gene in lung adenocarcinoma. *Cell Death Dis* 2021;12:424—39.
18. Montes M, Nielsen MM, Maglieri G, et al. The lncRNA MIR31HG regulates p16INK4A expression to modulate senescence. *Nat Commun* 2015;6:6967—81.
19. Wang R, Ma Z, Feng L, et al. LncRNA MIR31HG targets HIF1A and p21 to facilitate head and neck cancer cell proliferation and tumorigenesis by promoting cell-cycle progression. *Mol Cancer* 2018;17:162—7.
20. Tu C, Ren X, He J, et al. The predictive value of lncRNA MIR31HG expression on clinical outcomes in patients with solid malignant tumors. *Cancer Cell Int* 2020;20:115—27.
21. Lin SC, Liu CJ, Ji SH, et al. The upregulation of oncogenic miRNAs in swabbed samples obtained from oral premalignant and malignant lesions. *Clin Oral Investig* 2021. https://doi.org/10.1007/s00784-021-04108-y.
22. Zhou Y, Zhou B, Pache L, et al. Metascape provides a biologist-oriented resource for the analysis of systems-level datasets. *Nat Commun* 2019;10:1523—32.
23. Fernandez NF, Gundersen GW, Rahman A, et al. Clustergrammer, a web-based heatmap visualization and analysis tool for high-dimensional biological data. *Sci Data* 2017;4:170151—62.
24. Liu CJ, Tsai MM, Hung PS, et al. Mir-31 ablates expression of the HIF regulatory factor FIH to activate the HIF pathway in head and neck carcinoma. *Cancer Res* 2010;70:1635—44.
25. Chang KW, Hung WW, Chou CH, et al. LncRNA MIR31HG drives oncogenicity by inhibiting the limb-bud and heart development gene (LBH) during oral carcinoma. *Int J Mol Sci* 2021;22:8383.
26. Wu B, Zhang XJ, Li XG, Jiang LS, He F. Long non-coding RNA LOC344887 is a potential prognostic biomarker in non-small cell lung cancer. *Eur Rev Med Pharmacol Sci* 2017;21:3808—12.
27. Hung SY, Lin CC, Hsu CL, et al. The expression levels of long non-coding RNA KIAA0125 are associated with distinct clinical and biological features in myelodysplastic syndromes. *Br J Haematol* 2021;192:589—98.
28. Chen JF, Wu P, Xia R, et al. STAT3-induced lncRNA HAGLROS overexpression contributes to the malignant progression of gastric cancer cells via mTOR signal-mediated inhibition of autophagy. *Mol Cancer* 2018;17:6—21.
29. Zhou K, Xu J, Yin X, Xia J. Long noncoding RNA HAGLROS promotes cell invasion and metastasis by sponging miR-152 and upregulating ROCK1 expression in osteosarcoma. *Comput Math Methods Med* 2020;2020:7236245.
30. Li K, Sun D, Gou Q, et al. Long non-coding RNA LINC00460 promotes epithelial-mesenchymal transition and cell migration in lung cancer cells. *Cancer Lett* 2018;420:80—90.
31. Li J, Huang S, Zhang Y, Zhuo W, Tong B, Cai F. LINC00460 enhances bladder carcinoma cell proliferation and migration by modulating miR-612/FOXK1 axis. *Pharmacology* 2021;106:79—90.
32. Su Y, Wu H, Pavlosky A, et al. Regulatory non-coding RNA: new instruments in the orchestration of cell death. *Cell Death Dis* 2016;7:e2333.
33. Fagerberg L, Hallström BM, Oksvold P, et al. Analysis of the human tissue-specific expression by genome-wide integration of transcriptomics and antibody-based proteomics. *Mol Cell Proteom* 2014;13:397—406.
34. Zhou Y, Fan Y, Zhou X, et al. Significance of lncRNA MIR31HG in predicting the prognosis for Chinese patients with cancer: a meta-analysis. *Biomark Med* 2020;14:303—16.
35. Eide PW, Eilertsen IA, Sveen A, Lothe RA. Long noncoding RNA MIR31HG is a bona fide prognostic marker with colorectal cancer cell-intrinsic properties. *Int J Cancer* 2019;144:2843—53.
36. Hinske LC, Galante PA, Kuo WP, Ohno-Machado L. A potential role for intragenic miRNAs on their hosts' interactome. *BMC Genom* 2010;11:533—45.
37. Roepman P, Wessels LF, Kettelarij N, et al. An expression profile for diagnosis of lymph node metastases from primary head and neck squamous cell carcinomas. *Nat Genet* 2005;37:182—6.
38. Lu WC, Kao SY, Yang CC, et al. EGF up-regulates miR-31 through the C/EBPβ signal cascade in oral carcinoma. *PLoS One* 2014;9:e108049.
39. Yang H, Liu P, Zhang J, et al. Long noncoding RNA MIR31HG exhibits oncogenic property in pancreatic ductal adenocarcinoma and is negatively regulated by miR-193b. *Oncogene* 2016;35:3647—57.